Monitoring and Controlling System to Artificial Habitat of Antlion (Myrmeleon Sp.) based Wireless Sensor Network

Fairuz Rahmadika[1], Aad Hariyadi[2], Lis Diana Mustafa[3]
[1,2,3] Digital Telecommunication Network Study Program,
Department of Electrical Engineering, State Polytechnic of Malang, Indonesia
[2,3] Telecommunication Engineering Study Program,
Department of Electrical Engineering, State Polytechnic of Malang, Indonesia
[1]1841160057@student.polinema.ac.id, [2]aad.hariyadi@polinema.ac.id, [3]lis.diana@polinema.ac.id

***Abstract*—Antlion habitat that breeders create currently does not use a system that can protect the habitat from changes in temperature and humidity. In addition, when they are about to be sold, breeders filter and sort the antlion one by one. Therefore, a system is made that can monitor and control changes in temperature and humidity as well as harvesting automatically through the application. This system is designed using a wireless sensor network with temperature and humidity sensors DHT22, IR MLX90614 with light actuators and mist makers as well as loadcell sensors to trigger off the sieving motor which is connected to the Firebase database and interface Flutter aplication. Based on the results of testing the accuracy of temperature, humidity, infrared, and loadcell sensor readings, respectively, they are 98.07, 97.58%, 98.38%, 98.78% with an average delay 216.97ms can maintain temperature changes in the range 24-30°C and humidity in the range 70-80% stably. And the average value of harvest time is 30.37 seconds with an average decrease in sand load of 56.7 grams when the harvesting mechanism is running.**

***Keywords*— Antlion, Wireless Sensor Network, DHT22, IRMLX90614, Loadcell**

I. INTRODUCTION

Antlion is a type of insect which in the larval stage contains the active substance sulfonylurea which is useful in the treatment of Diabetes Mellitus (DM) [1]. The antlions habitat is in dry sandy areas with a temperature range of 24-30°C and humidity of 70-80% so that changes in temperature and humidity are critical parameters for the chance of antlions living [2]. However, the monitoring and control of these two parameters has not been carried out by retreat breeders. In addition, the harvesting process carried out by farmer still uses manual sorting by using a sieve in each larval burrow so that it takes a relatively long time [3]. Based on these problems, an effort is needed to maintain the availability of antler larvae and facilitate the harvest process. Therefore, it is necessary to have a technology-based monitoring and control system to maintain the survival of the retreat and facilitate the harvest process.

Utilization of technology related to temperature and humidity monitoring and control systems through microcontroller devices refers to research [4] and [5], which uses the DHT22 temperature and humidity sensor and the MLX90614 IR infrared temperature sensor with outputs active or deactivated lamp and mist makers actuator that can be accessed via smartphones for easy monitoring. The system created works by integrating sensors and actuators with the ESP8266 microcontroller. The choice of this type of microcontroller is because it is able to transmit data with a communication line that was originally directly to the router using an IP Address, now it can use a MAC Address with a longer available transmission distance [6][7]. This things to support the habitat of farmers who are far from internet access. The addition of a semi-automatic sifting harvest system with a function to sort the antlions larvae that are ready to harvest. Therefore, a system is made that can monitor and control temperature and humidity, as well as a harvesting mechanism in the antlions habitat.

II. METHOD

A. System design

The system design contains a block diagram design with antlion habitat references. The block diagram is shown in Fig. 1.

Explanations of the components on the block diagram include:

1. Nodes are 2 retreat habitats with habitat configurations to the receiver to the microcontroller to firebase and the cloud so that they can be accessed via smartphones.
2. The sender microcontroller is used as a center for controlling sensors and actuators as well as transmitting data connected to the receiver microcontroller wirelessly.
3. Inputs include a DHT22 sensor for temperature and humidity detection, MLX90614 IR sensor for sand surface temperature detection, and Loadcell sensor for sand load detection when the sieving system is active.
4. Output includes Relay as an electronic switch to control the on and off the motor. Mist maker-24 Volt DC fan for humidity control and lights for temperature control in the retreat habitat.

The results of the interview determine the use of a star topology based on the location of the undur-undur habitat breeder in Grobyog, Tj. Rejo, Wuluhan, Jember with habitat data shown in Table I [3], [7], [8].

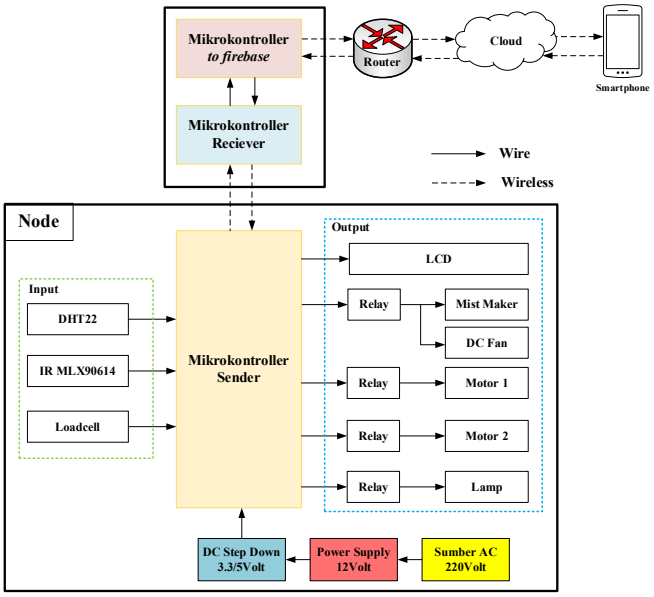

Figure 1 Blok Diagram System

TABLE I
ANTLION OBSERVATION DATA

Temperature (°C)	Humidity (%)	Medium	Harvest	Antlion Size
24 – 30	70 – 80	Dry sand	±3 Week	±4-5mm

Table I shows the data from the observation of the crab crab habitat in the breeder with parameters of temperature and humidity, habitat media, harvest time and size of crab cakes that are ready to be sold.

B. *Flowchart*

The flowchart contains the design flow of the sensor monitoring system for controlling temperature and humidity as well as the harvest mechanism system. The sensor monitoring flow chart is shown in Fig. 2.

The flowchart of the temperature, humidity and feed monitoring system design has 2 habitat monitoring parameters, namely the average temperature and humidity. The average temperature condition is obtained from the calculation of the average value between the air temperature and the surface temperature of the sand, the results of which will control the on and off lights according to the provisions. Humidity is the humidity of the air in the habitat area, the reading of which will control the mist maker on and off according to the provisions. Each of these conditions will also run on habitats 1 and 2 which will then be displayed via the LCD and sent to the server to be displayed via the smartphone application.

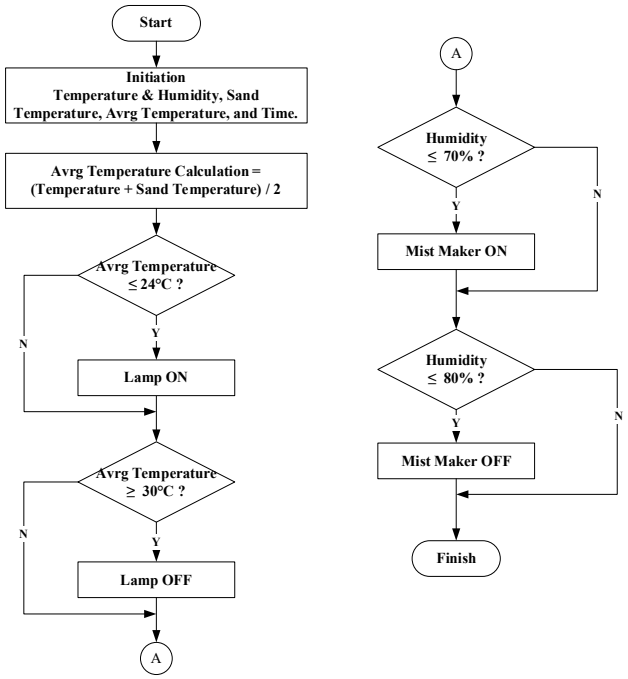

Figure 2 Flowchart Monitoring Sensor

The flowchart of the harvesting mechanism system is shown in Fig. 3.

This sifting system design flowchart has 2 sieving mechanism parameters, namely harvest and load. Harvest conditions will determine for active control of motor 1 (opening the shelf base) and motor 2 (sifter). The load condition is the weight of the sand that falls into the shelter, the reading of which will determine the control of motor 2 (sifter) and motor 1 (closing the rack base). Each of these conditions will be carried out on the habitat to be harvested or also used to determine the difference in sand load which will determine the increase in the population of crabs. The sieving mechanism can be run through a smartphone or directly through the sieving button on the habitat.

C. *Prototype design*

The prototype design shows the design of the use and placement of sensors, actuators and microcontrollers in the artificial turtle habitat.

The following is a description of Fig. 4:

1. **A** shows the lamp actuator for temperature control.
2. **B** shows the temperature and humidity sensor, namely DHT22.
3. **C** using a sand surface temperature sensor, namely IR MLX90614.
4. **D** indicates the weight sensor for sand falling into the holding container using the loadcell on the LED scale.
5. **E** shows the ESP8266 microcontroller as the control center between sensors and actuators.
6. **F** show the driving motor of the sieving mechanism.
7. **G** shows the driving motor of the pedestal opening and closing mechanism.
8. **H** show mist maker actuator for humidity control.
9. **I** show LCD.

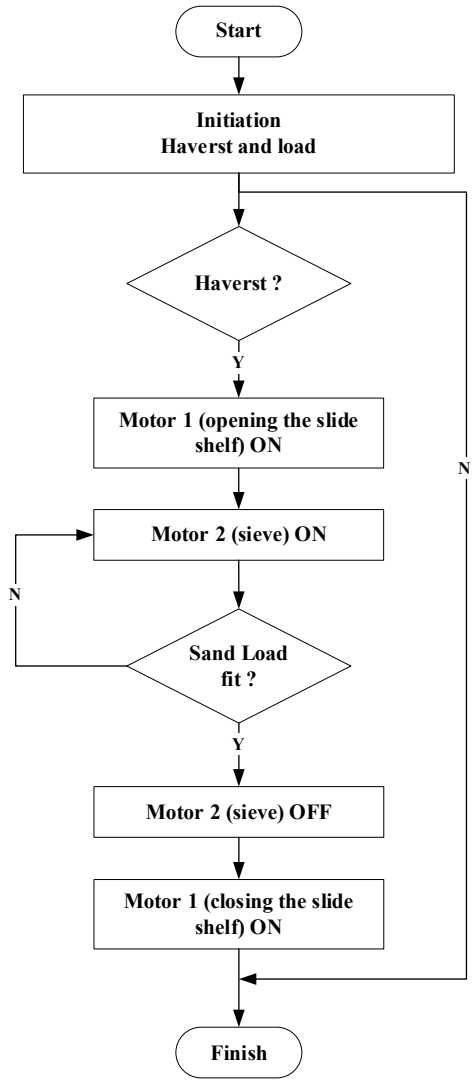

Figure 3 Flowchart Monitoring Sensor

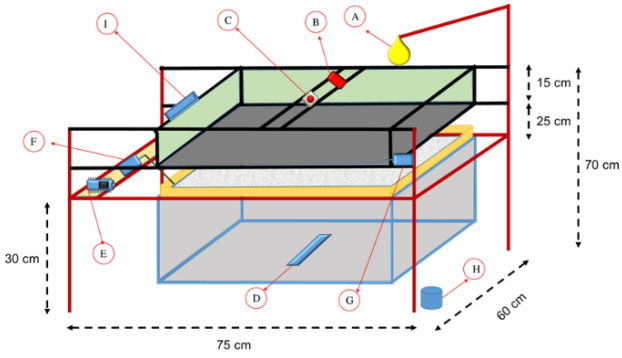

Figure 4 Prototype Design

The implementation of the component design is shown in Fig. 5.

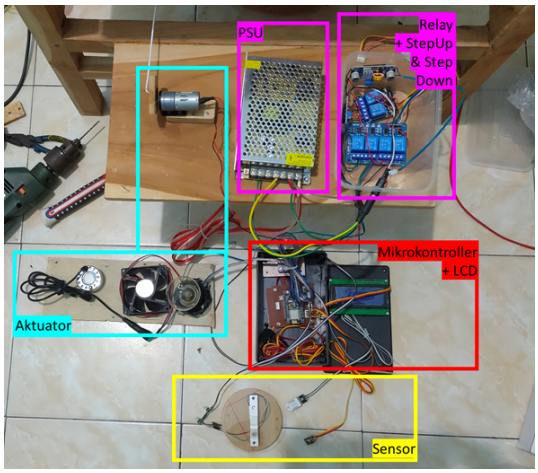

Figure 5 Implementation of Component Design

III. RESULTS AND DISCUSSION

Based on the planning of the system, testing is carried out to determine its performance and analyze the results of the design. So that it can find out the results of several test parameters.

A. Sensor Test

Sensor testing is carried out to determine the accuracy of the sensor reading value compared to the reading on a standardized measuring instrument. This test was carried out on three sensors used in the system, including the DHT22 sensor as a temperature sensor, IR MLX90614 as a humidity sensor and loadcell as a load sensor. Sensor test results are shown in the Table II.

TABLE II
DHT22 TEMPERATURE SENSOR ACCURACY TEST RESULTS

DHT22 (°C)	Thermometer (°C)	Deviasi Error (%)
26.8	26.2	2.290076336
27.5	26.7	2.996254682
25.4	26.3	3.422053232
28.1	27.5	2.181818182
26.8	26.9	0.383141762
25.7	26.1	1.486988848
26.2	26.9	2.651515152
26	26.4	1.53256705
25.7	26.1	1.509433962
26.3	26.5	0.754716981

Based on the results of the temperature sensor test in Table II, it is known that there is a difference in the temperature value of the DHT22 reading compared to the value on the UNI-T333S Thermometer so that the deviation error value is obtained. Furthermore, the error deviation value is used as a reference to determine the average error value and accuracy of the DHT22 sensor through the following calculations:

$$Error\ Average = \frac{19.20856619}{10}\ x\ 100\%$$

$$= 1.920856619\%$$

$$Accuracy = 100\% - (1.920856619\%) = 98.07914338\%$$

From the calculation of the temperature sensor accuracy, the accuracy value is 98.08%. These results indicate that the

temperature sensor is of high accuracy because it has a reading error of below 3% with an accuracy specification on the DHT22 datasheet of ± 0.5℃ [9].

TABLE III
IR MLX90614 SURFACE TEMPERATURE ACCURACY TEST RESULTS

IRMLX90614 (℃)	Thermogun (℃)	Error (%)
32.59	31.7	2.807570978
25.43	25.2	0.912698413
26.19	26.06	0.49884881
25.9	25.7	0.778210117
27.29	26.9	1.449814126
26.73	25.8	3.604651163
27.15	26.9	0.92936803
25.7	26.2	1.908396947
30.87	31.6	2.310126582
31.3	31.6	0.949367089

Based on the test results of the temperature sensor in Table III, it is known that there is a difference in the temperature value of the MLX90614 IR reading compared to the value of the Thermogun Infrared GM320 so that the deviation error value is obtained. Furthermore, the error deviation value is used as a reference to determine the average error value and accuracy of the MLX90614 IR sensor through the following calculations:

$$Error\ Average = \frac{16.14905225}{10}\ x\ 100\%$$

$$= 1.614905225\%$$

$$Accuracy = 100\% - (1.614905225\%) = 98{,}38509477\%$$

From the calculation of the temperature sensor accuracy, the accuracy value is 98.38%. These results indicate that the temperature sensor is of high accuracy because it has a reading error of below 3% with an accuracy specification on the IR MLX90614 datasheet of ± 2.56℃ [10].

TABLE IV
DHT22 HUMIDITY SENSOR ACCURACY TEST RESULTS

DHT22 (%)	Hygrometer (%)	Error (%)
80.3	78.7	2.033036849
80	78.9	1.394169835
79.9	78.1	2.304737516
82.7	80.1	3.245942572
81.6	80.4	1.492537313
78.2	80.7	3.097893432
77.7	78.6	1.145038168
79.8	77.7	2.702702703
79.2	76.9	2.990897269
77.9	75.1	3.728362184

Based on the results of the temperature sensor test in Table IV, it is known that there is a difference in the temperature value of the DHT22 reading compared to the value on the UNI-T333S Hygrometer so that the deviation error value is obtained. Furthermore, the error deviation value is used as a reference to determine the average error value and humidity accuracy of the DHT22 sensor through the following calculations:

$$Error\ Average = \frac{24.13531784}{10}\ x\ 100\%$$

$$= 2.413531784\%$$

$$Accuracy = 100\% - (2.413531784) = 97.58646822\%$$

From the calculation of the humidity sensor accuracy, the accuracy value is 97.58%. These results indicate that the humidity sensor includes high accuracy because it has a reading error below 3% with an accuracy specification on the DHT22 datasheet of ± 5% [9].

TABLE V
LOADCELL SENSOR ACCURACY TEST RESULTS

Loadcell (g)	Scales (g)	Error (%)
295.34	300	1.553333333
491.66	500	1.668
998.63	1000	0.137
1481.58	1500	1.228
1981.85	2000	0.9075
2474.59	2500	1.0164
3453.32	3500	1.333714286
3944.81	4000	1.37975
4931.35	5000	1.373
6401.71	6500	1.512153846

Based on the load sensor test results in Table V, it is known that there is a difference in the load value of the Loadcell reading compared to the value on the Digital Scales so that the error deviation value is obtained. Furthermore, the error deviation value is used as a reference to determine the average error value and accuracy of the Loadcell sensor through the following calculations:

$$Error\ Average = \frac{12.10885147}{10}\ x\ 100\%$$

$$= 1.210885147\%$$

$$Accuracy = 100\% - (1.210885147) = 98.78911485\%$$

From the calculation of the load sensor accuracy, the accuracy value is 98.79%. These results indicate that the load sensor includes high accuracy because it has a reading error below 3% [11].

B. Sensor Monitoring Results

The sensor monitoring results display the temperature and humidity sensor values as well as the surface temperature for 24 hours to determine the active and inactive conditions of the lamp and mistmaker-fan actuator.

Based on Table VI, it is known that there is a change in the value of air temperature, sand surface temperature and the average value of both and the value of humidity after monitoring for 24 hours. The results of this temperature monitoring are used to determine the temperature value that can activate or deactivate the lights in each habitat. Meanwhile, the results of humidity monitoring are used as information on whether the mistmaker-fan is on or off. The data displayed shows changes in temperature and humidity values in habitat 1 with a relatively long time span. This is caused by the design of the habitat that is not closed and the selection of specifications for lamp actuators and mist makers that are not in accordance with the shape of the habitat. To find out more

clearly the temperature changes in habitat 1, see the graph in Fig. 6.

TABLE VI
MONITORING SENSOR DATA OF HABITAT 1

Time	Habitat 1			
	Sand Temperature (°C)	Temperature (°C)	∑ Temperature (°C)	Humidity (%)
06.00	22.52	23.81	23.165	76.71
07.00	24.04	24.21	24.125	75.61
08.00	25.48	25.71	25.595	72.51
09.00	25.26	25.01	25.135	74.31
10.00	25.06	25.21	25.135	71.11
11.00	25.48	27.71	25.595	68.51
12.00	28.18	27.11	27.645	67.11
13.00	29.2	30.11	29.655	65.71
14.00	30.1	30.61	30.355	64.71
15.00	28.12	28.71	28.415	69.41
16.00	26.94	27.01	26.975	70.21
17.00	25.74	26.11	25.925	73.51
18.00	24.22	24.61	24.415	71.01
19.00	23.78	24.11	23.945	73.21
20.00	24.9	24.31	24.605	74.51
21.00	24.58	23.91	24.245	74.91
22.00	24.72	23.31	24.015	77.01
23.00	24.66	23.71	24.185	76.71
24.00	24.52	24.71	24.615	75.91
01.00	23.94	24.31	24.125	76.11
02.00	24.22	24.81	24.515	80.11
03.00	23.98	24.11	24.045	74.51
04.00	24.4	24.11	24.255	77.81
05.00	24.18	24.01	24.095	76.81

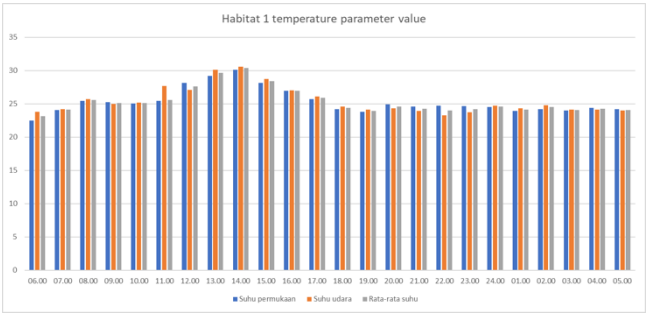

Figure 6 Temperature Change Graph

In the graph of changes in habitat temperature 1 displays the surface temperature and air temperature parameters from the IR sensor readings MLX90614 and DHT22. The two parameters will determine the average temperature value that functions to activate and deactivate the lamp actuator. The system is activated at 06.00 with the readings of the surface temperature of the sand and the air temperature are 22.52°C and 23.81°C respectively resulting in an average temperature of 23.165°C which will activate the lamp actuator because the average temperature value is <24°C. The lamp will be kept active until 14.00 because after that time there is an increase in temperature >30°C where the surface temperature of the sand and the detected air temperature are 30.1°C and 30.61°C, respectively, resulting in an average temperature of 30.355°C. Furthermore, the lamp actuator will turn on again at 19.00 because the surface temperature of the sand and the detected air temperature are 23.78°C and 24.11°C, respectively, resulting in an average temperature of 23.945°C which is <24°C. Based on the results of temperature monitoring, it is known that the system can run according to the conditions that have been set, namely the light actuator is active when the temperature is <24°C and is disabled when >30°C.

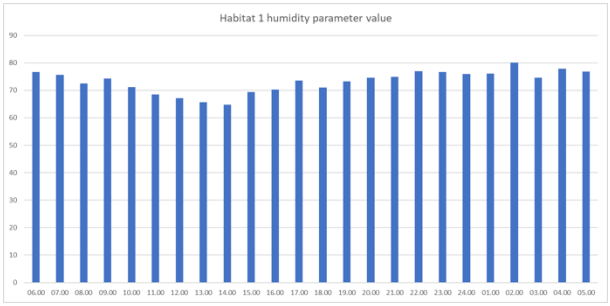

Figure 7 Humidity Change Graph

In the graph of changes in habitat humidity 1 shows the humidity parameters for activating and deactivating the mist maker-fan actuator. The system is activated at 06.00 with a humidity reading of 76.71% so that the fan actuator and mist maker are still in an inactive condition because the humidity value is between 70-80%. Based on the graph, the mist maker-fan starts to activate at 11.00 because the humidity value is 68.51% and remains active until 02.00 because the humidity value has exceeded 80%, which is 80.11%. In accordance with the results of the humidity parameter, you can turn on the mist maker and fan according to the conditions set in the system, namely the mist maker and fan turn on when the humidity is <70% and turn off when <80%.

C. Harvest Mechanism Results

The harvesting mechanism is activated when the snails enter the ready-to-harvest age, which is ± 3 weeks. At harvest time, the button from the application is pressed so that input 1 is sent to the firebase and read by the microcontroller to start moving the motor, opening the lid of the habitat mat and the sieving motor. Sand that is in the habitat will go down to the side of the sifter when the bottom is open. The sifted sand will be accommodated into a container equipped with a loadcell sensor so that the sand load value will be detected as a trigger to deactivate the base opening and closing motor and the sieving motor. In this case, the weight of the sand after sieving must match the weight of the sand before the sieving process so that the weight of this sand can be used as a parameter for making the trigger off. The results of the harvest mechanism include Loadcell load sensor readings with indicators of deactivation of motor actuators 1 and 2.

TABLE VII
HARVEST MECHANISM TEST

Time	Button Status	Loadcell (gram)	Motor
20.47.15	OFF	-2,65	Inactive
20.47.46	ON	4747,10	Active
15.51.34	OFF	-5,71	Inactive
15.52.10	ON	4671,98	Active
16.07.25	OFF	- 2,13	Inactive
16.07.59	ON	4633,7	Active

Table VII shows the test data of the harvest mechanism with load and time parameters. In the first test with a total load of 4747.10 grams consisting of 500 grams of container load and 4247.10 grams of sand load, the working mechanism time is 31 seconds. In the second test, the total load data was 4671.98 grams consisting of 500 grams of container load with 4171.98 grams of sand so that the mechanism working time was 26 seconds. In the third test, data obtained for a total load of 4633.70 grams consisting of 500 grams of container load with 4133.70 grams of sand load with a mechanism working time of 34 seconds. Based on the test results, it is known that the average value of harvest time is 30.37 seconds with an average decrease in sand load of 56.7 grams.

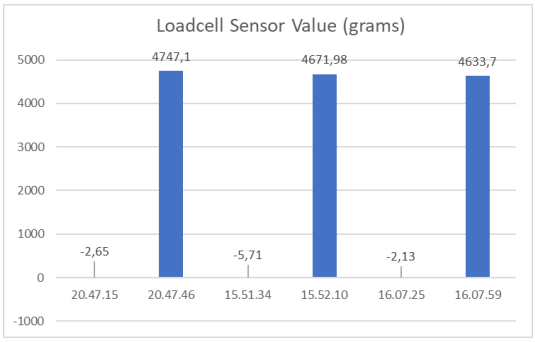

Figure 8 Loadcell Sensor Value Graph

Fig. 8 shows the results of the graph of measuring the value of the sand load before and after harvest in accordance with the data listed in Table VII. Based on these data there are differences in the value of the sand load for each test. The average sand load read by the loadcell sensor in each test is 4684.26 grams with an average load reduction of 56.7 grams. The reduction in load is caused when the motor moves when the harvesting mechanism is active causing vibrations, so that there is sand spilled around the habitat.

D. Application Results

The results of the application display the flutter application menu along with system functionality that was previously connected to the firebase database so that it is integrated into the microcontroller system [12]. The Flutter application can be accessed via a smartphone connected to the internet as shown in Fig. 9. As can observed the dashboard menu displays sensor data on habitat 1 which consists of the values of surface temperature, air temperature and humidity as well as an on/off button for the harvest mechanism. The value of each sensor will change after ± 10 seconds so that farmers can monitor changes in temperature and humidity without looking directly at the location of the crab's habitat. Temperature data will be collected in the "FORM" menu data log to display a graph of fluctuations in temperature and humidity values. When the "ON/OFF" button is pressed, the system will automatically run the harvesting mechanism and send information to the database to be forwarded to the microcontroller [13]. After the load sensor detects the trigger, the information will be sent back to the database and forwarded to the application as a trigger OFF button.

Figure 9 Dashboard menu

E. Data communication test results

TABLE VIII
TESTING OF TRANSMISTION DISTANCE MAC ADDDRESS AND IP ADDRESS

Distance (m)	Mac Address (Board 1 to Receiver)	IP Address (Receiver to WiFi)
1	Delivery Success	Connected
5	Delivery Success	Connected
10	Delivery Success	Connected
20	Delivery Success	Failed Connection Lost
30	Delivery Success	Failed Connection Lost
50	Delivery Success	Failed Connection Lost
80	Delivery Success	Failed Connection Lost
90	Delivery Fail	Failed Connection Lost
100	Delivery Fail	Failed Connection Lost

Based on Table VIII it can be seen the capacity of the transmission distance between the two communication lines through directional or point to point testing. In this system, data transmission using IP Address communication lines is the transmission line of the receiver's microcontroller to WiFi, the maximum stable transmission distance is 10 meters. While the data transmission system through the MAC Address communication line is a habitat microcontroller to a receiver microcontroller, the maximum stable transmission distance is 80 meters. In this case, the MAC Address communication path on the ESP8266 has a longer transmission capability than the IP Address so that it can support habitat conditions that are far from internet access.

- Delay

Delay is the transmission time of packets from the microcontroller to the database and vice versa [14]. The calculation of the delay value uses the formula for the difference between the time the packet is received and the time the packet is sent according to the formula:

$$delay = (time\ received - time\ sent)$$

$$average\ delay = \frac{total\ delay}{total\ packet}$$

$$average\ delay = \frac{4556{,}41677}{21} = 216{,}9722271\ ms$$

- Packet loss

Packet loss is the number of packets lost during the transmission process [14].

$$packet\ loss = (\frac{packet\ sent - packet\ receive}{packet\ receive})\ x\ 100$$

$$packet\ loss = \left(\frac{302 - 301}{301}\right) x\ 100 = 0.33\%$$

Based on testing using the Wireshark application for 7 days of testing, the average daily delay is 216,9722271 ms which is included in the good category in the TIPHON standard. Meanwhile, in the packet loss test, the average daily packet loss is 0.33% which is included in the very good category in the TIPHON standard[15].

IV. CONCLUSION

Sensors of air temperature, surface temperature and humidity with an accuracy of 98.08%, 98.38%, 97.58%, respectively, can control the temperature range of 24-30℃ and humidity range of 70-80 quite stable. The loadcell sensor with an accuracy of 98.78% can regulate the inactivity of the sieving motor when the sand load value is >4000 grams. The average load reading is 4684.26 grams with an average time span of 30.37 seconds with a reduction in the sand load per harvest by an average of 56.7 grams. ESP8266 microcontroller data communication MAC Address transmission line has a range of up to 80 m while the IP Address is only 10 m. The average daily delay obtained is 216.9722271ms in the good category with an average daily packet loss of 0.33% in the very good category.

REFERENCES

[1] D. H. Susanto, R. W. Kartika, P. H. Heng, A. W. Santoso, V. M. Lopulalan and A. Wijaya, "Pengaruh Ekstrak Undur-undur (Myrmeleon sp) terhadap Glukosa Darah dan Hematokrit pada Tikus Diabetes," Jurnal Ilmiah Kedokteran Wijaya Kusuma, vol. 9, no. 2, p. 209=2017, 2020.

[2] V. Widyawati, Ampuhnya Lintah dan Undur-undur Tebas Beragam Penyakit, Yogyakarta: Laksana, 2019.

[3] Z. Abiddin, Interviewee, Yusron Herbamart Wuluhan, Kabupaten Jember. [Interview]. 25 05 2022.

[4] A. Wiranto and H. Nurwarsito, "Sistem Monitoring Pengatur Suhu dan Kelembaban pada Kandang Jangkrik berbasis Internet of Things (Studi Kasus Budidaya Jangkrik Perorangan di Kabupaten Blitar)," Jurnal Pengembangan Teknologi Informasi dan Ilmu Komputer, vol. 6, pp. 2673-2680, 2022.

[5] M. Babiuch, P. Foltýnek and P. Smutný, "Using the ESP32 Microcontroller for Data Processing," International Carpathian Control Conference (ICCC) IEEE, pp. 1-6, 2019.

[6] W. Puspitasari and H. Y. Perdana R, "Real-Time Monitoring and Automated Control of Greenhouse Using Wireless Sensor Network: Design and Implementation," 2018 International Seminar on Research of Information Technology and Intelligent Systems (ISRITI), 2018, pp. 362-366, doi: 10.1109/ISRITI.2018.8864377.

[7] M. Arundina, S. Ngabekti and K. Santoso, "Kesintasan Undur-Undur pada Media Aklimatisasi," Biosaintifika: Journal of Biology & Biology Education, vol. 6, no. 1, pp. 18-23, 2014.

[8] K. Miler, B. E. Yahya and M. Czarnoleski, "Substrate moisture, particle size and temperature preferences of trap-building larvae of sympatric antlions and wormlions from the rainforest of Borneo," Ecological Entomology, vol. 44, no. 4, pp. 488-493, 2019.

[9] F. Puspasari, T. P. Satya, U. Y. Oktiawati, I. Fahrurrozi and H. Prisyanti, "Analisis Akurasi Sistem Sensor DHT22 berbasis Arduino terhadap Thermohygrometer Standar," JURNAL FISIKA DAN APLIKASINYA, vol. 16, no. 1, pp. 40-45, 2020.

[10] I. Inayah, "Analisis Akurasi Sistem Sensor IR MLX90614 dan Sensor Ultrasonik berbasis Arduino terhadap Termometer Standar," Jurnal Fisika Unand (JFU), vol. 10, no. 4, pp. 428-434, 2021.

[11] F. Y. Saputra, M. S. Al Amin and Perawati, "Alat Pengukur Tinggi Badan, Berat Badan, Dan Suhu Badan Digital Menggunakan Sensor Ultrasonik, Load Cell, Dan Inframerah Mlx90614," Jurnal Tekno, vol. 19, no. 1, pp. 60-67, 2022.

[12] R. Juliana, K. N. VG, R. G and S. P, "Evecurate – A Smart Event Management App Using Flutter and Firebase," International Journal of Scientific Research & Engineering Trends, vol. 7, no. 4, pp. 2519-2524, 2021.

[13] R. H. Y. Perdana, H. Hudiono and A. F. N. Luqmani, "Water Leak Detection and Shut-Off System on Water Distribution Pipe Network Using Wireless Sensor Network," 2019 International Conference on Advanced Mechatronics, Intelligent Manufacture and Industrial Automation (ICAMIMIA), 2019, pp. 297-301, doi: 10.1109/ICAMIMIA47173.2019.9223386.

[14] P. R. Utami, "Analisis Perbandingan Quality Of Service Jaringan Internet Berbasis Wireless Pada Layanan Internet Service Provider (ISP) Indihome dan Fist Media," Jurnal Ilmiah Teknologi dan Rekayasa, vol. 25, no. 2, pp. 125-137, 2020.

[15] Subektiningsih, Renaldi and P. Ferdiansyah, "Analisis Perbandingan Parameter QoS Standar TIPHON Pada Jaringan Nirkabel Dalam Penerapan Metode PCQ," Explore, vol. 1, no. 57-63, p. 12, 2022.